Excitable behavior can explain the "ping-pong" mode of communication between cells using the same chemoattractant

Andrew B. Goryachev[1)2)*], *Alexander Lichius*[2)3)], *Graham D. Wright*[2)4)] *and Nick D. Read*[2)]

Here we elucidate a paradox: how a single chemoattractant-receptor system in two individuals is used for communication despite the seeming inevitability of self-excitation. In the filamentous fungus *Neurospora crassa*, genetically identical cells that produce the same chemoattractant fuse via the homing of individual cell protrusions toward each other. This is achieved via a recently described ''ping-pong'' pulsatile communication. Using a generic activator-inhibitor model of excitable behavior, we demonstrate that the pulse exchange can be fully understood in terms of two excitable systems locked into a stable oscillatory pattern of mutual excitation. The most puzzling properties of this communication are the sudden onset of oscillations with final amplitude, and the absence of seemingly inevitable self-excitation. We show that these properties result directly from both the excitability threshold and refractory period characteristic of excitable systems. Our model suggests possible molecular mechanisms for the ping-pong communication.

Keywords:
cell-cell communication; cell signaling; excitable behavior; mathematical modeling; *Neurospora crassa*

DOI 10.1002/bies.201100135

[1)] Centre for Systems Biology, University of Edinburgh, Edinburgh, UK
[2)] Institute of Cell Biology, University of Edinburgh, Edinburgh, UK
[3)] Current Address: Department of Microbiology, Center for Scientific Research and Higher Education of Ensenada (CICESE), Ensenada, Baja California, Mexico
[4)] Current Address: Institute of Medical Biology, A*STAR, Singapore

***Corresponding author:**
Andrew B. Goryachev
E-mail: andrew.goryachev@ed.ac.uk

Abbreviations:
CAT, conidial anastomosis tube; **cAMP,** cyclic adenosine monophosphate; **GFP,** green fluorescent protein.

Supporting information online

Introduction

Chemotaxis and chemotropic growth are ubiquitous among all forms of life [1–3]. They play an important role in the physiology of simple unicellular organisms, such as bacteria and yeasts [4–6], as well as within our own complex multicellular bodies, e.g. during development, wound healing or the immune response [7]. If a chemical signal released by one cell is sensed by another, they can use chemotaxis to meet each other. Most often, such an invitation is not specific: all cells capable of sensing the signal are invited and welcome to join the party. Thus, starved *Dictyostelium* amoebas secrete cyclic adenosine monophosphate (cAMP) whose gradient they follow to assemble into compact cell aggregates [8, 9].

A different situation occurs if a cell needs to meet only one partner, e.g. when two haploid individuals seek each other to mate and form a diploid zygote. In this case finding the correct mating partner is possible because they have distinct genetic makeups. Thus, budding yeasts have two mating types, $\boldsymbol{a}$ and $\boldsymbol{\alpha}$, that secrete their own mating pheromones and express receptors for the pheromones of the opposite type [10]. However, in many fungi, including the filamentous ascomycete *Neurospora crassa*, individual cells also fuse for reasons other than reproduction.

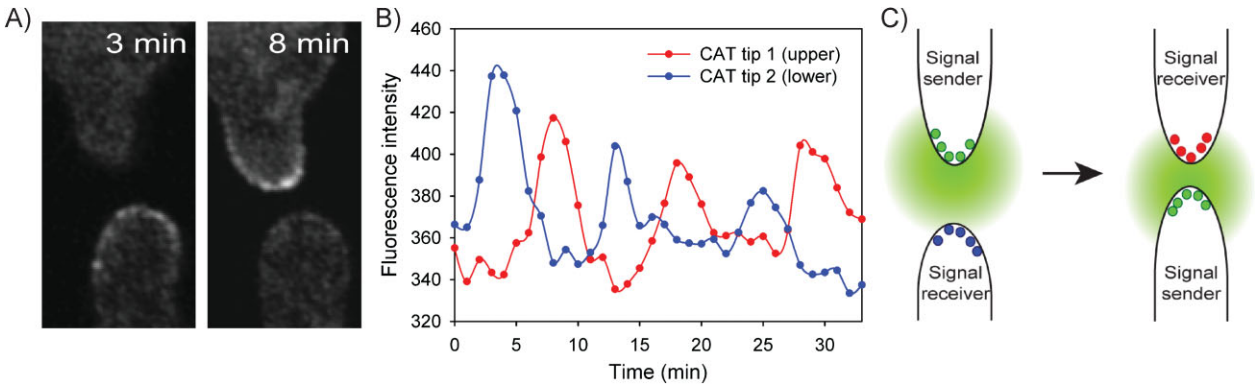

Figure 1. The ping-pong signaling between two *Neurospora* cells that grow chemotropically toward each other. **A:** Fluorescent signal of MAK-2 MAP kinase labeled with GFP at the tips of cell protrusions. Two time frames separated by half a period correspond to the first two peaks on panel B. **B:** Time series of the total tip MAK-2-GFP fluorescence quantified for the two cells shown in A. **C:** Cartoon illustrating the principle of the alternating exchange of signaling pulses. The MAK-2-GFP localization is shown as blue filled circles in one cell and red in the other to match the notations in panel B, while green filled circles correspond to SO localization. The green regions outside the cells represent the field of diffusing chemoattractant produced by the cell that sends the signal. CAT – conidial anastomosis tube, a specialized cellular protrusion destined for fusion with other cells.

Shortly after germination, asexual spores (conidia) of *Neurospora* develop small, slender protrusions termed conidial anastomosis tubes (CATs) [11] that seek each other and fuse tip-to-tip to join the individual conidial germlings into a supercellular colony-network [12, 13]. Being genetically and developmentally identical, CATs have to rely on the communication involving a common, as yet unidentified, chemoattractant. Such a mode of communication, sometimes called "self-signaling" [13], poses an unexpected biophysical challenge. Indeed, the signal released by the cell itself is always stronger than the remote partner's signal, which is inevitably weakened by diffusion. How such a mode of communication might be functional despite the seemingly inevitable auto-excitation remained a puzzling paradox up until recently.

From microscopic observations it was nevertheless clear that chemical communication between CATs indeed takes place. The CATs select their partners at a distance as evidenced by their purposeful homing toward each other that becomes apparent when their separation is less than ~15 μm. Genetic analyses identified a number of candidate genes whose products were required for CAT formation, homing and fusion [14–19]. Deletion of the gene encoding the MAP kinase MAK-2 resulted in cells unable to chemotropically home and fuse with other, even normal, wild-type, cells. To shed light on the cellular localization of this kinase, Fleißner et al. [20] genetically tagged MAK-2 with green fluorescent protein (GFP). Unexpectedly, they found that in the CATs undergoing chemotropic homing, MAK-2 localized to the plasma membrane at the CAT tips periodically in time, reaching maximum intensity every 10–12 min (see Fig. 1A). Importantly, the exact location of the maximal intensity of MAK-2-GFP signal within the tip was predictive of the future direction of CAT turning, suggesting a direct causative link between the MAP kinase signaling and the direction of growth. The apparent MAK-2 oscillations in the homing CATs are always shifted by half a period, so that peaks in one pattern correspond to troughs in the other and vice versa as shown in Fig. 1B (see also Supporting information movies[1]). Remarkably, another essential protein for CAT fusion, with unknown function, soft (SO) [17], exhibited a complementary oscillatory pattern, with a maximum intensity in one cell synchronized with the maximum of MAK-2 in the other. Fleißner et al. [20] suggested that the MAK-2 peaks correspond to the receiving of a signal while the SO maxima to the sending of it (see Fig. 1C). The observed dynamics of MAK-2 and SO then indicates that the two CATs alternately exchange signaling pulses as if throwing each other a ball; thus, this communication mode was named the "ping-pong" signaling mechanism [13].

How does such a synchronized pattern suddenly emerge upon reaching some critical intercellular distance? What mechanisms are responsible for it? In the present contribution we present a simple model of the pulsatile signaling and argue that the observed behavior of *Neurospora* CATs can be well explained by the concept of biological excitability. A biological system responds excitably to an external signal if at first it rapidly amplifies the signal and then, with a delay, it suppresses the response to return back to the resting state in which it existed before the signal. The latter phase is often referred to as perfect adaptation (see, e.g., [3]). Excitable behavior has long been studied in neuroscience, as well as in chemistry and physics. Following this well-developed framework we formulate a number of experimentally testable hypotheses regarding the nature of the molecular mechanisms that underlie ping-pong signaling.

[1] Supporting information movies 1 and 2 show MAK-2-GFP localization in CATs homing toward each other and then fusing. Two 36 min image sequences were recorded at 2 min intervals. Each frame consists of a projection of 6 images captured as a z stack (acquired every 0.5 μm over a 3 μm range) and then deconvolved.

Excitable behavior

The ability to perform a sudden, transient burst of activity in response to a super-threshold stimulus is a fundamental property of many biological systems. In order to exhibit such dynamics, however, a system need not be as complex as a living organism. A lightning bolt that hits a solitary tree has a good chance to ignite it. The resulting fire, if caught, will rage until it consumes the whole tree and will extinguish itself once it runs out of the combustible wood. All excitable systems possess the critical excitation threshold that the external stimulus needs to exceed in order to produce the response and the refractory period that follows immediately after the period of activity. During this refractory period the system is unable to respond to another stimulus, regardless of its amplitude. All excitable systems, however, eventually recover and stay poised for another burst of activity to be unleashed by a super-threshold stimulus whenever it arrives. In our example, if a new tree grows on the place of the burned one, it again can catch fire should a lightning strike the same spot twice.

In a dense forest, however, a single burning tree will very likely ignite its neighbors. The fire will then sweep through the forest like a wave, leaving in its wake ash and cinder. The ability to directionally relay the activity pulse makes a spatially distributed system consisting of excitable elements a suitable medium for the propagation of information. Not surprisingly, the concept of excitability emerged in biology in the context of nerve pulse propagation [21–26]. In 1952 Hodgkin and Huxley [27] developed an elaborate electro-chemical model that for the first time described the initiation and propagation of the action potential along the axon. Following in their steps, Fitzhugh (1961) and, independently, Nagumo et al. (1962) proposed a highly simplified model that is commonly used in the literature as a prototypical model of excitability [28, 29]. The concept of excitability has since firmly established itself in a number of biological disciplines. Thus, most of the intracellular Ca^{2+} signals [30–32] and cardiac muscle contraction [33–35] can be described as propagating waves of excitation. Bursts of cAMP released by individual aggregating *Dictyostelium* amoebas self-organize into the excitable spiral waves that rotate around the aggregation center [36–38]. The discovery of excitable dynamics in chemical reactions [39], of which the famous Belousov-Zhabotinsky reaction is perhaps the most notable example, also fuelled interest in the excitability outside of biology. Numerous theoretical and computational studies inspired by the experimental results provided us with the presently comprehensive mathematical understanding of this phenomenon.

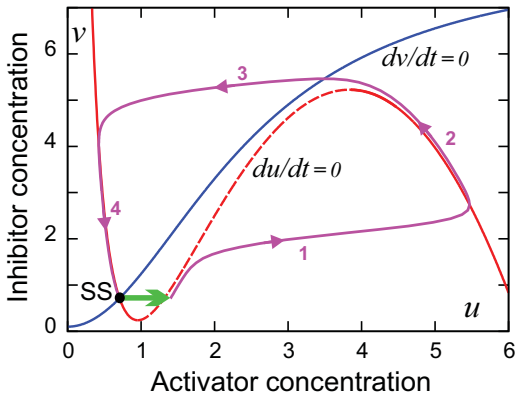

Figure 2. Phase portrait of a prototypical activator-inhibitor model illustrating the concept of excitable behavior. The nullclines of the system are shown by red and blue curves. A typical excitable phase trajectory is shown by the magenta curve. SS – steady state, green arrow symbolizes a super-threshold stimulus that induces the excitable behavior. Numbers on the trajectory correspond to the four phases of excitable dynamics discussed in the text. Model parameter values: $\varepsilon = 1$, $\alpha = -12.4$, $\beta = 8.05$, $\gamma = 8$, $k = 6$, $u_0 = 5.6$, $v_0 = 0.1$.

The essence of excitable behavior can be captured mathematically with a simple model that uses ordinary differential equations to describe the concentrations of two hypothetical substances, activator A and inhibitor I [40]. The activator rapidly amplifies itself and increases the production of the inhibitor, while the inhibitor slowly suppresses the activator, e.g. by increasing its degradation. We stipulate that the concentrations of A and I should be positive at all times and also that in the absence of any stimulation the system should rest in a steady state characterized by small concentrations of A and I. This can be achieved by appropriately modifying the prototypical Fitzhugh-Nagumo (FHN) model, e.g., as follows:

$$\begin{cases} \dot{u} &= u_0 - \alpha u + \beta u^2 - u^3 - vu \\ \dot{v} &= \varepsilon\left(v_0 + \gamma \dfrac{u^2}{u^2 + K} - v\right) \end{cases}$$

where, for convenience, the concentrations of A and I are denoted as u and v.

Since the FHN model is the simplified and mathematically condensed version of the Hodgkin-Huxley model, its terms lost clear connection to biophysical processes.

A typical example of the excitable behavior in this model is shown in Fig. 2. On the phase plane (u, v), the positions where the concentrations of A or I do not change in time are given by the so-called nullclines, the curves where $\dot{u} = 0$ or $\dot{v} = 0$, respectively. Since, by definition, in a steady state neither concentration changes, the only steady state (u_{ss}, v_{ss}) of our model lies at the intersection of the two nullclines.

The time evolution of the model with arbitrary initial conditions u^*, v^* is represented on the phase plane by a smooth curve, known as phase trajectory, that starts at the point (u^*, v^*) and ends at (u_{ss}, v_{ss}). The sigmoid-shaped activator nullcline $\dot{u} = 0$, shown in Fig. 2 by the red line, plays a special role in the dynamics of the model.

The two branches of the nullcline with negative slope (solid line) are said

Hypotheses

to be stable and attractive because phase trajectories initiated in various points tend to approach these branches and then run close to them on the way to the steady state. On the contrary, the central positively sloped segment (dashed line) is unstable and repels phase trajectories so that the trajectories started on either side of the dashed line rapidly turn away from it. Therefore, if the model dynamics is initiated at the position lying to the left of the unstable segment of the activator nullcline, the phase trajectory of the system will approach the left attractive branch of the nullcline and will move along it until it eventually reaches the steady state. If, however, the initial position lies to the right of the unstable segment, the trajectory will first leap toward the right attractive branch. It will follow this branch upwards until the bend in the nullcline and only then jump to the left branch along which it will continue down to the steady state (cf. Fig. 2). This model, therefore, provides a simple pictorial illustration to the concept of the super-threshold stimulus that is required to excite the system. Indeed, any sudden change in the steady state concentrations of A and I that throws the system across the activator nullcline (green arrow in Fig. 2) will produce a dramatic burst of activity. From the arrival of the stimulus until the return to the steady state, the phase trajectory of the excitable system can be approximately subdivided into four segments. First, the activator is rapidly produced while the concentration of I increases only slightly. On the second segment, the concentration of A, after reaching its maximal value, drops by a fraction. At the same time a significant amount of the inhibitor is produced. On the third segment, both concentrations diminish. However, the drop in the concentration of A is significantly larger. During the final fourth segment of the trajectory the inhibitor is degraded and the concentration of the activator slightly increases back to its steady state value. The last two segments approximately correspond to the refractory period of the system.

The model

We are now in a position to formulate a simple heuristic model that could explain the pulsatile interaction between two cells that respond to the same pheromone, such as a pair of *Neurospora* CATs. The activator-inhibitor module described above can be used as the core intracellular element responsible for the excitable behavior. We leave the discussion of the molecular identities of the hypothetical activator and inhibitor to the following section. Here, we simply postulate that the intracellular dynamics of the CATs is described by two sets of variables (u_1, v_1) and (u_2, v_2) that represent the concentrations of the activator and inhibitor in CAT1 and CAT2, respectively. To enable communication between the CATs, we first need to model the secretion of the chemoattractant molecule. Following the current consensus [41], we assume that the secretory vesicles are produced by the Golgi complex at some constant rate. Using molecular motors these vesicles travel along the cytoskeletal elements to the tip of the CAT protrusion and dock at the plasma membrane. Docked vesicles then can fuse with the plasma membrane and their contents released into the surrounding medium. In the steady state, when no excitable behavior takes place, vesicles should be produced, transported to the tip, docked and emptied at some basal rate to enable continuous background signaling. To produce a *burst* of secretion, however, it is absolutely necessary that the secretory pathway is controlled by the activator-inhibitor module. For the sake of concreteness, we postulate that the inhibitor does not play an active role, while the activator increases the probability of vesicle docking and, at the same time, suppresses their fusion and chemoattractant release. As a result, during the activator pulse a large number of docked vesicles would accumulate at the CAT tip standing at the ready to be fused with the membrane as soon as the concentration of A drops sufficiently low to allow it.

Since it takes only a fraction of a second for a small molecule to cross an ~10 μm gap between the homing cells, we assume diffusion of the signaling molecules in the extracellular medium to be practically instantaneous. Therefore, the signal is sensed by both CATs simultaneously, as soon as it is released. Denoting the populations of the free cytoplasmic vesicles and vesicles docked at the plasma membrane as w and x, respectively, we obtain the model equation that describes the dynamics of the first CAT

$$\begin{cases} \dot{u}_1 = u_0 - \alpha u_1 + \beta u_1^2 - u_1^3 - v u_1 + \underbrace{k_3\left(\frac{u_{ss}}{u_1}\right)^3 x_1}_{\text{auto-excitation}} + \underbrace{k_4\left(\frac{u_{ss}}{u_2}\right)^3 x_2}_{\text{CAT2 signal}} \\ \dot{v}_1 = \varepsilon\left(v_0 + \gamma\frac{u_1^2}{u_1^2 + K} - v_1\right) \\ \dot{w}_1 = \underbrace{w_0}_{\text{vesicle production}} - \underbrace{k_1\left(\frac{u_1}{u_{ss}}\right)^2 w_1}_{\text{vesicle docking}} \\ \dot{x}_1 = \underbrace{k_1\left(\frac{u_1}{u_{ss}}\right)^2 w_1}_{\text{vesicle docking}} - \underbrace{k_2\left(\frac{u_{ss}}{u_1}\right)^3 x_1}_{\text{vesicle fusion - signal release}} \end{cases}$$

Here, u_{ss}, the steady state concentration of the activator, is introduced into the equations to ascertain that the activator does not affect the secretory pathway at the steady state. The two terms at the end of the first equation describe the self-excitation and excitation by the second CAT. Since, as mentioned above, the concentration of the chemoattractant secreted by the cell itself is always higher at its own surface, we assume that the coupling parameter k_3 is greater than k_4. The equations for the remaining four variables (u_2, v_2, w_2, x_2) that describe the second CAT can be written by simply transposing indexes "1" and "2" of the variables in the equations above.

To simulate the communication between two *Neurospora* CATs, we induce one of them, which in the follow-

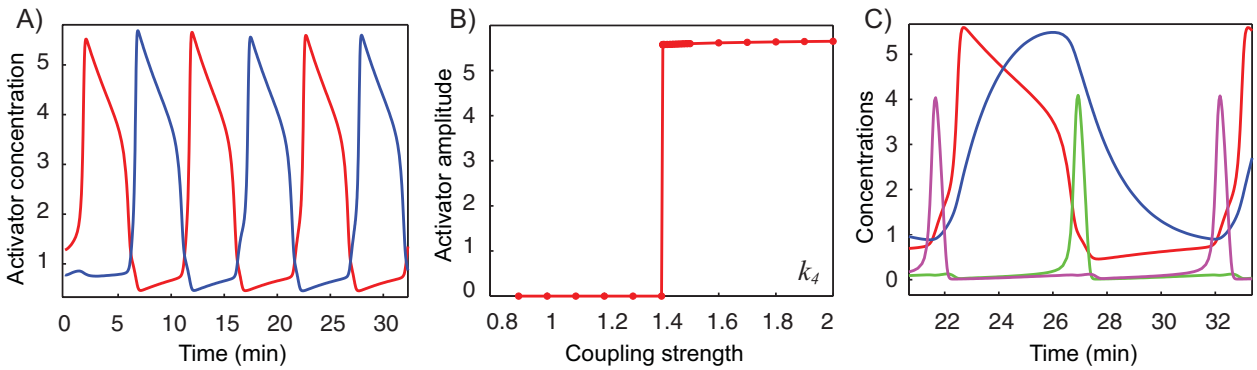

Figure 3. A simple model of the ping-pong communication between two CATs. **A:** A periodic pattern of pulse exchange emerges in response to a single pulse from CAT1 (red). The time series of the activator dynamics in CAT1 and CAT2 is shown by red and blue curves, respectively. **B:** The ping-pong pulsatile pattern emerges suddenly with the final amplitude at the critical intercellular separation. The maximal amplitude of the steady state activator time series is plotted versus the coupling parameter k_4 that symbolizes the intercellular separation. At $k_4 = 2.0$, the intercellular coupling is equal to the self-interaction, $k_4 = k_3$. Thus, this represents CATs in direct physical contact. **C:** One full period of ping-pong dynamics. The time series of the activator (red), inhibitor (blue), and the signal secretion (green) of one CAT are shown together with the inducing secretory pulses of the opposite CAT (magenta). Model parameter values: $\varepsilon = 0.55$, $u_{ss} = 0.7542$, $k_1 = 0.1$, $k_2 = 1.0$, $k_3 = 2.0$, $k_4 = 1.5$, $w_0 = 1$; other parameters as indicated in Fig. 2.

ing we refer to as CAT1, to undergo a single burst of activity and then follow the ensuing behavior of both CATs. The change in the intercellular distance is symbolized in our model by the variation of the coupling strength k_4.

Therefore, when the cells are far apart (small k_4), CAT1 produces a single burst to which CAT2 does not respond. Within some critical "distance", however, the ping-pong mode of communication establishes robustly as shown in Figure 3A. After a few unequal transient exchanges, the pulsing activity falls into a stable periodic pattern that continues infinitely long suggesting that the system reached a stable attracting state. Thus, while each CAT in isolation is an excitable system that requires a super-threshold excitation stimulus, the two of them, if positioned sufficiently close, form an autonomous oscillator. Comparing Figs. 1B and 3A we notice that our simple model fully reproduces the experimentally observed pattern with the strict half-a-period shift between the two cells that establishes instantaneously, without any detectable synchronization period that would have been necessary should the oscillations have been cell-autonomous. Moreover, without any additional effort, we recover another experimental result – the sudden character of the communication establishment.

Figure 3B shows the dependence of the stationary amplitude of the CAT1 activator signal on the coupling strength k_4, hence, the intercellular distance. Unexpectedly, we see that the ping-pong mode emerges suddenly with full amplitude that grows only slightly upon further increase in k_4. This remarkable property can be understood if we recall that the excitable behavior can be induced only if the stimulus exceeds a certain finite threshold [40].

The detailed anatomy of the ping-pong communication is revealed in Figure 3C that presents approximately one complete period of the steady state periodic dynamics.

The cycle starts with the CAT2 secretion pulse (magenta) that sends the activator (red) and inhibitor (blue) in CAT1 on their loop of excitable dynamics. As the concentration of the activator drops, the release of chemoattractant from CAT1 is triggered. Comparison of Figs. 2 and 3C shows that at the peak of the signal release, CAT1 is in the middle of its refractory period when the concentration of the inhibitor is high and, therefore, any possibility of self-excitation is precluded. This delay in the secretory pulse is the fundamental prediction of the model. Should the release occur earlier in the activator-inhibitor cycle, not only would it result in partial self-excitation but also it would bring about the premature firing of CAT2 whose signal would reach CAT1 during its refractory period thus breaking the ping-pong pattern.

Interestingly, a conceptually similar model was proposed by Höfer et al. [42] as an explanation for the "chemotactic wave paradox" in *Dictyostelium* [43]. In this model, amoebas move up the gradient in the rising front of the incoming wave of cAMP but still in the wake of the departing wave due to the desensitization of the chemotactic receptors. Both models resolve their respective paradoxes by suggesting advantageous synchronization of the periodicities of the external signal and the intracellular dynamics. However, in our system, this synchronization arises automatically via the exchange of pulses and does not require that the system parameters be tuned to achieve the desired synchronization.

Potential molecular mechanisms

Armed with the hypothesis regarding the dynamic nature of the ping-pong signaling, we laid the foundation for the interpretation of the existing experimental results. More importantly, our model provides experimentally testable predictions that point toward the missing pieces of the puzzle. Results of genetic knockout studies have so far revealed a surprising paucity of genes apparently involved in the mechanism [19]. While some genes likely evaded the screens, these results nevertheless suggest that the hypothetical ping-pong mechanism may involve relatively few key components.

MAK-2 MAP kinase is the best candidate for the role of activator

It is possible that the activity of several components downstream of the signal receptor may jointly play the role of activator. However, direct comparison of the experimental data with the behavior of the model (cf. Figs. 1B and 3A) suggests that the activator is the active phosphorylated form of MAP kinase MAK-2. This conjecture is strongly supported by the results of experiments with the analog-sensitive mutant of MAK-2 whose activity can be turned off by addition of the cell-permeable drug 1NM-PP1. Not only did this drug prevent the periodic localization of MAK-2-GFP to the cell tips, but it also stopped the chemotropic growth of CATs toward each other, indicating that MAK-2 is not just a downstream component of the signaling.

Is the inhibitor absolutely necessary?

The identity of the hypothetical inhibitor is more elusive. In fact, no such substance may exist in reality. Indeed, another possible realization of the excitable module is based on the activator-substrate scheme [40]. In this instance effective inhibition of the activator is achieved by depletion of the substrate that is used up during the activator pulse and needs replenishing before the system can undergo another burst of activity. The activator-substrate mechanisms appear to be more commonly realized in real chemical and biological systems (think again of our forest fire example) and the identity of the substrate, however unexpected, is typically deduced from the concrete biochemical mechanism (see further discussion below). Thus, in a model of cell polarity establishment in budding yeast, the substrate turned out to be represented by the same protein as the activator, yet in its alternate, inactive state [44].

Slow mechanisms based on gene transcription are likely not involved

As the diffusible signal and its receptor remain unknown, it is hard to approach the unraveling of the molecular mechanism systematically, from the bottom up. Yet, some conclusions that narrow down the domain of search can be drawn. Thus, the observed period of the ping-pong exchange, $\sim$10 min, suggests that feedback mechanisms involving gene transcription with typical characteristic time of $\sim$1 hour [45] are likely not directly involved in the excitable behavior. Indeed, Fleißner et al. treated homing CATs with protein synthesis inhibitor cycloheximide and found that this drug did not affect the advanced stage of pulse exchange [20]. This result may indicate that the excitable mechanism solely relies on the cell signaling processes that take place on the membrane and in the cytoplasm of growing CATs.

Fast positive feedback loops are necessary for rapid signal amplification

Could the excitable behavior emerge solely from the dynamics of the NRC-1-MEK-2- MAK-2 MAP kinase cascade? To build an excitable module with the required temporary kinetics, it is necessary to have very fast (response time $<$1 min) positive feedback loop(s) for the rapid amplification of the incoming signal and slower, but still fast (characteristic time 5–10 min) negative feedback loops for termination of the response. While very little is known about the specific MAP kinase cascade in question, results from yeast and several mammalian systems suggest that all the required feedback loops could be indeed embedded within the dynamics of the MAP kinase cascade itself. Thus, recent work in budding yeast suggested that the homolog of MAK-2, Fus3, phosphorylates and inhibits its own inhibitor, phosphatase Msg5 [46, 47]. Pre-coupling of MAK-2 to its de-activating phosphatase via direct binding could provide both the necessary activation threshold and the ability to rapidly ramp up the activity of the MAPK once the phosphatase is phosphorylated and detached from the kinase (see Fig. 4A).

Other pathways could be also involved in the rapid amplification of MAK-2 activity.

Interestingly, the *Neurospora* MAPKKK NRC-1 contains a putative Ras-binding domain. Therefore, like its fission yeast homolog, Byr2, NRC-1 could be an effector of Ras. In budding yeast, MAP kinase Kss1 phosphorylates and activates Ras GEF, Cdc25 [48]. Therefore, it is feasible that MAK-2 auto-amplifies its activity by promoting activation of Ras that in turn activates the MAP kinase cascade (Fig. 4B).

Intermediate speed negative feedback loops are required for perfect adaptation

Potential negative feedback mechanisms, capable of terminating MAK-2 signaling within the required time scale, are also not in short supply [49, 50]. For example, in budding yeast both Fus3 and Kss1 phosphorylate their upstream kinase Ste7 which inhibits the activity of the cascade via dissociation of Ste7 from the signaling complex [51]. Fus3 also phosphorylates its MAPKKK Ste11 [52]. Several yeast MAPK cascades are known to include scaffolding proteins, such as Ste5 and Ste50, whose phosphorylation by the MAPK further contributes to the disassembly of the signaling cascades [53] (Fig. 4C). While the ubiquitination and eventual degradation of thus phosphorylated proteins are important for the long-term repression of MAPK cascades, they are likely too slow to contribute to the ping-pong dynamics. At the same time, the disassembly of a MAPK cascade resulting from the hyperphosphorylation of its components by the respective MAP kinase is possibly the most universal fast downregulation mechanism [54] that is also found in mammalian systems [55]. Returning to the discussion of the identity of the hypothetical substrate, we can propose that either an upstream kinase or, as yet unidentified, scaffolding protein in their active, not inhibited by MAK-2 phosphorylation, state could fill in this role.

MAK-2 could regulate both docking and fusion of secretory vesicles

Perhaps the most interesting prediction of our model is the requirement that the activator, putatively MAK-2, controls secretion of the chemoattractant. The first regulatory phase, increased docking of the secretory vesicles, may have a simple molecular explanation. In fungi, vesicles are typically tethered to the plasma membrane via the exocyst complex that is a direct effector of small Rho GTPases, in particular, Cdc42 [41]. Activation of the *Neurospora* Cdc42 or

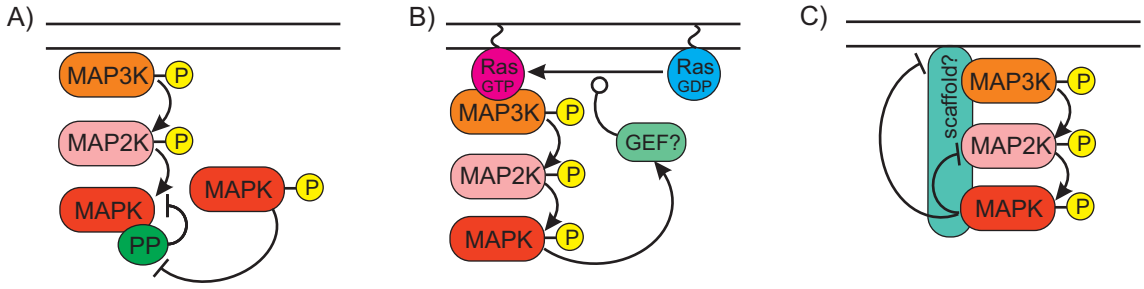

Figure 4. Potential feedback mechanisms that could convert the MAK-2 MAP kinase cascade into an excitable system. **A:** Pre-coupling of MAK-2 to a protein phosphatase (PP) could apply a brake to the activation of the cascade. If the activated MAK-2 phosphorylates and dissociates the phosphatase, it would then generate a rapid positive feedback loop. **B:** If the most upstream MAP cascade kinase MAP3K (NRC-1) is an effector of Ras, another positive feedback loop is possible via phosphorylation and activation by MAK-2 of an unidentified Ras GEF. **C:** Possible negative feedback loops acting through the disassembly of the cascade after hyperphosphorylation of the upstream kinase MAP2K (MEK-2) and a hypothetic cascade scaffold by MAK-2. For generality the kinases of the MAP cascade are denoted by their functional roles (MAP2K – MAP kinase kinase, MAP3K – MAP kinase kinase kinase). Activated status of the kinases is shown symbolically by the presence of a phosphate group. Horizontal double line represents the membrane bilayer.

possibly its close homolog Rac by MAK-2 could, in fact, kill two birds with one stone – enhance vesicle docking and control the direction of growth at the same time. The hypothesized inhibition of vesicle fusion by MAK-2 is currently more nebulous, but might involve the direct phosphorylation of the fusion machinery, e.g. proteins, by MAK-2. While the exact molecular function of SO protein remains enigmatic, our model suggests that it might be involved in the signal release phase. Interestingly, sequence alignment shows a very weak homology of SO to the proteins of aczonin/piccolo family. In mammalian synapses, these proteins are thought to regulate the transition of neurotransmitter-loaded vesicles from the reserve to the release-ready pool and thus are involved in the coordination of rapid fusion of multiple vesicles [56].

Conclusions

In biology, excitability has long been assumed to pertain to the electrophysiological activity in certain specialized cell types of higher organisms. Recent progress in the experimental techniques and methods that allows us to observe finer intracellular events on faster time scales has called for the revision of this outdated paradigm. A cell need not be "excitable" in the above sense to exhibit excitable behavior on intracellular spatial scales and during certain phases of its life cycle. The generic recipe for excitability – rapidly amplify the incoming signal, slowly suppress the response – includes a wealth of known biological phenomena into the category of "excitable behavior". Indeed, many biological systems from yeast and *Dictyostelium* amoebas to human cells respond to various extracellular signals in this way [3, 54].

So, does labeling these phenomena as "excitable" result in mere proliferation of terminology? Far from this, it unlocks the conceptual and methodological riches of physics and chemistry, where the phenomenon of excitability had been well understood in abstract terms of simplified activator-inhibitor and activator-substrate models. In this contribution we considered chemotactic communication between genetically identical cells that rely on the same pheromone (self-signaling). We concluded that the transition from the steady chemoattractant release to the exchange of pulse-like releases, as observed in the filamentous fungus *Neurospora crassa*, solves a seemingly inevitable problem of auto-excitation that is inherent in self-signaling. Indeed, in our model the release of chemoattractant coincides with the refractory period of the intracellular activator-inhibitor loop, during which excitable systems are known to be insensitive to the incoming stimuli.

Most of the molecules and their interactions that underlie the ping-pong mechanism remain unknown. However, armed with the hypothesis of the excitable nature of this mechanism, we can inform further experimentation and avoid costly blind searching in fruitless domains. This can be achieved by directing the experiment toward the molecular mechanisms with desired outcome, e.g. positive or negative feedback loops, and specific dynamical properties, such as the characteristic time of the feedback loop activation. Mutually enriching interaction between experiment and modeling will undoubtfully elucidate both the molecular mechanisms and the dynamical principles of ping-pong signaling.

References

1. **Rappel W-J**, **Loomis WF.** 2009. Eukaryotic chemotaxis. *Wiley Interdiscip Rev Syst Biol Med* **1**: 141–9.
2. **Iglesias PA**, **Devreotes PN.** 2008. Navigating through models of chemotaxis. *Curr Opin Cell Biol* **20**: 35–40.
3. **Levchenko A**, **Iglesias PA.** 2002. Models of eukaryotic gradient sensing: application to chemotaxis of amoebae and neutrophils. *Biophys J* **82**: 50–63.
4. **Krell T**, **Lacal J**, **Munoz-Martinez F**, **Reyes-Darias JA**, et al. 2011. Diversity at its best: bacterial taxis. *Environ Microbiol* **13**: 1115–24.
5. **Rao CV**, **Ordal GW.** 2009. The molecular basis of excitation and adaptation during chemotactic sensory transduction in bacteria. *Contrib Microbiol* **16**: 33–64.
6. **Leeder AC**, **Palma-Guerrero J**, **Glass NL.** 2011. The social network: deciphering fungal language. *Nat Rev Microbiol* **9**: 440–51.
7. **Stephens L**, **Milne L**, **Hawkins P.** 2008. Moving towards a better understanding of chemotaxis. *Curr Biol* **18**: R485–94.
8. **Garcia GL**, **Parent CA.** 2008. Signal relay during chemotaxis. *J Microsc* **231**: 529–34.
9. **Loomis WF.** 2008. cAMP oscillations during aggregation of *Dictyostelium*. *Adv Exp Med Biol* **641**: 39–48.

10. **Arkowitz RA.** 2009. Chemical gradients and chemotropism in yeast. *Cold Spring Harb Perspect Biol* **1**: a001958.
11. **Roca GM**, **Arlt J**, **Jeffree CE**, **Read ND.** 2005. Cell biology of conidial anastomosis tubes in *Neurospora crassa*. *Eukaryot Cell* **4**: 911–9.
12. **Read ND**, **Fleißner A**, **Roca MG**, **Glass NL.** 2010. Hyphal fusion. In Borkovich KA, Ebbole D, eds; *Cellular and Molecular Biology of Filamentous Fungi*. Washington DC: American Society of Microbiology.
13. **Read ND**, **Lichius A**, **Shoji J**, **Goryachev AB.** 2009. Self-signalling and self fusion in filamentous fungi. *Curr Opin Microbiol* **12**: 608–15.
14. **Aldabbous MS**, **Roca MG**, **Stout A**, **Huang IC**, et al. 2010. The ham-5, rcm-1 and rco-1 genes regulate hyphal fusion in *Neurospora crassa*. *Microbiology* **156**: 2621–9.
15. **Xiang Q**, **Rasmussen C**, **Glass NL.** 2002. The ham-2 locus, encoding a putative trans membrane protein, is required for hyphal fusion in *Neurospora crassa*. *Genetics* **160**: 169–80.
16. **Pandey A**, **Roca GM**, **Read ND**, **Glass NL.** 2004. Role of a mitogen-activated protein kinase pathway during conidial germination and hyphal fusion in *Neurospora crassa*. *Eukaryot Cell* **3**: 348–58.
17. **Fleißner A**, **Sarkar S**, **Jacobson DJ**, **Roca GM**, et al. 2005. The so locus is required for vegetative cell fusion and postfertilization events in *Neurospora crassa*. *Eukaryot Cell* **4**: 920–30.
18. **Simonin AR**, **Rasmussen CG**, **Yang M**, **Glass NL.** 2010. Genes encoding a striatin-like protein (ham-3) and a forkhead associated protein (ham-4) are required for hyphal fusion in *Neurospora crassa*. *Fungal Genet Biol* **47**: 855–68.
19. **Fu C**, **Iyer P**, **Herkal A**, **Abdullah J**, et al. 2011. Identification and characterization of genes required for cell-to-cell fusion in *Neurospora crassa*. *Eukaryot Cell* **10**: 1100–9.
20. **Fleißner A**, **Leeder AC**, **Roca MG**, **Read ND**, et al. 2009. Oscillatory recruitment of signaling proteins to cell tips promotes coordinated behaviour during cell fusion. *Proc Natl Acad Sci USA* **106**: 19387–92.
21. **Altamirano M**, **Coates CW**, **Grundfest H.** 1955. Mechanisms of direct and neural excitability in electroplaques of electric eel. *J Gen Physiol* **38**: 319–60.
22. **Mueller P.** 1958. On the kinetics of potential, electromotance, and chemical change in the excitable system of nerve. *J Gen Physiol* **42**: 193–229.
23. **Sato K.** 1959. On the ''transforming action'' related to the threshold, chronaxie and accommodation constant of a living excitable system. *Jpn J Physiol* **9**: 327–35.
24. **Tobias JM.** 1960. Further studies on the nature of the excitable system in nerve. I. Voltage-induced axoplasm movement in squid axons. II. Penetration of surviving, excitable axons by proteases. III. Effects of proteases and of phospholipases on lobster giant axon resistance and capacity. *J Gen Physiol* **43**: 57–71.
25. **Mueller P**, **Rudin DO**, **Tien HT**, **Wescott WC.** 1962. Reconstitution of cell membrane structure in vitro and its transformation into an excitable system. *Nature* **194**: 979–80.
26. **Tobias JM**, **Agin DP**, **Pawlowski R.** 1962. The excitable system in the cell surface. *Circulation* **26**: 1145–50.
27. **Hodgkin AL**, **Huxley AF.** 1952. A quantitative description of membrane current and its application to conduction and excitation in nerve. *J Physiol* **117**: 500–44.
28. **Fitzhugh R.** 1961. Impulses and physiological states in theoretical models of nerve membrane. *Biophys J* **1**: 445–66.
29. **Nagumo J**, **Arimoto S**, **Yoshizawa S.** 1962. An active pulse transmission line simulating nerve axon. *Proc IRE* **50**: 2061–70.
30. **Amundson J**, **Clapham D.** 1993. Calcium waves. *Curr Opin Neurobiol* **3**: 375–82.
31. **Sneyd J**, **Girard S**, **Clapham D.** 1993. Calcium wave propagation by calcium-induced calcium release: an unusual excitable system. *Bull Math Biol* **55**: 315–44.
32. **Berridge MJ.** 2002. The endoplasmic reticulum: a multifunctional signalling organelle. *Cell Calcium* **32**: 235–49.
33. **Winfree AT.** 1989. Electrical instability in cardiac muscle: phase singularities and rotors. *J Theor Biol* **138**: 353–405.
34. **Agladze K**, **Keener JP**, **Muller SC**, **Panfilov A.** 1994. Rotating spiral waves created by geometry. *Science* **264**: 1746–8.
35. **Winfree AT.** 2002. Chemical waves and fibrillating hearts: discovery by computation. *J Biosci* **27**: 465–73.
36. **Siegert F**, **Weijer CJ.** 1992. Three-dimensional scroll waves organize *Dictyostelium* slugs. *Proc Natl Acad Sci USA* **89**: 6433–7.
37. **Hofer T**, **Sherratt JA**, **Maini PK.** 1995. *Dictyostelium discoideum*: cellular self-organization in an excitable biological medium. *Proc Biol Sci* **259**: 249–57.
38. **Siegert F**, **Weijer CJ.** 1995. Spiral and concentric waves organize multicellular *Dictyostelium* mounds. *Curr Biol* **5**: 937–43.
39. **Kapral R**, **Showalter K.** 1995. *Chemical Waves and Patterns*. Dordrecht: Kluwer Academic Publishers. 648 p.
40. **Murray JD.** 2007. *Mathematical Biology*. New-York: Springer.
41. **Orlando K**, **Guo W.** 2009. Membrane organization and dynamics in cell polarity. *Cold Spring Harb Perspect Biol* **1**: a001321.
42. **Höfer T**, **Maini PK**, **Sherratt JA**, **Chaplan MAJ**, et al. 1995. Resolving the chemotactic wave paradox: a mathematical model for chemotaxis of *Dictyostelium* amoebae. *J Biol Syst* **3**: 967–73.
43. **Soll D**, **Wessels D**, **Sylvester A.** 1993. The motile behavior of amoebae in the aggregation wave in *Dictyostelium discoideum*. In Othmer HG, Maini PK, Murray JD, eds; *Experimental and Theoretical Advances in Biological Pattern Formation*. London: Plenum Press. pp. 325–38.
44. **Goryachev AB**, **Pokhilko AV.** 2008. Dynamics of Cdc42 network embodies a Turing-type mechanism of yeast cell polarity. *FEBS Lett* **582**: 1437–43.
45. **Hilioti Z**, **Sabbagh W Jr.**, **Paliwal S**, **Bergmann A**, et al. 2008. Oscillatory phosphorylation of yeast Fus3 MAP kinase controls periodic gene expression and morphogenesis. *Curr Biol* **18**: 1700–6.
46. **Flandez M**, **Cosano IC**, **Nombela C**, **Martin H**, et al. 2004. Reciprocal regulation between Slt2 MAPK and isoforms of Msg5 dual-specificity protein phosphatase modulates the yeast cell integrity pathway. *J Biol Chem* **279**: 11027–34.
47. **Marin MJ**, **Flandez M**, **Bermejo C**, **Arroyo J**, et al. 2009. Different modulation of the outputs of yeast MAPK-mediated pathways by distinct stimuli and isoforms of the dual-specificity phosphatase Msg5. *Mol Genet Genomics* **281**: 345–59.
48. **Cherkasova VA**, **McCully R**, **Wang Y**, **Hinnebusch A**, et al. 2003. A novel functional link between MAP kinase cascades and the Ras/cAMP pathway that regulates survival. *Curr Biol* **13**: 1220–6.
49. **Hao N**, **Behar M**, **Parnell SC**, **Torres MP**, et al. 2007. A systems-biology analysis of feedback inhibition in the Sho1 osmotic-stress-response pathway. *Curr Biol* **17**: 659–67.
50. **Feng Y**, **Davis NG.** 2000. Feedback phosphorylation of the yeast a-factor receptor requires activation of the downstream signaling pathway from G protein through mitogen-activated protein kinase. *Mol Cell Biol* **20**: 563–74.
51. **Maleri S**, **Ge Q**, **Hackett EA**, **Wang Y**, et al. 2004. Persistent activation by constitutive Ste7 promotes Kss1-mediated invasive growth but fails to support Fus3-dependent mating in yeast. *Mol Cell Biol* **24**: 9221–38.
52. **Esch RK**, **Errede B.** 2002. Pheromone induction promotes Ste11 degradation through a MAPK feedback and ubiquitin-dependent mechanism. *Proc Natl Acad Sci USA* **99**: 9160–5.
53. **Hao N**, **Zeng Y**, **Elston TC**, **Dohlman HG.** 2008. Control of MAPK specificity by feedback phosphorylation of shared adaptor protein Ste50. *J Biol Chem* **283**: 33798–802.
54. **Behar M**, **Hao N**, **Dohlman HG**, **Elston TC.** 2007. Mathematical and computational analysis of adaptation via feedback inhibition in signal transduction pathways. *Biophys J* **93**: 806–21.
55. **Fritsche-Guenther R**, **Witzel F**, **Sieber A**, **Herr R**, et al. 2011. Strong negative feedback from Erk to Raf confers robustness to MAPK signalling. *Mol Syst Biol* **7**: 489.
56. **Limbach C**, **Laue MM**, **Wang X**, **Hu B**, et al. 2011. Molecular in situ topology of Aczonin/Piccolo and associated proteins at the mammalian neurotransmitter release site. *Proc Natl Acad Sci USA* **108**: E392–401.